nature water

Article

https://doi.org/10.1038/s44221-024-00227-4

Simultaneous time-resolved inorganic haloamine measurements enable analysis of disinfectant degradation kinetics and by-product formation

Received: 10 November 2023

Accepted: 7 March 2024

Published online: 23 April 2024

Check for updates

Samuel H. Brodfuehrer[1,3], Daniel C. Blomdahl[1,3], David G. Wahman[2], Gerald E. Speitel Jr.[1], Pawel K. Misztal[1] & Lynn E. Katz[1]

We demonstrate the application of proton transfer time-of-flight mass spectrometry (PTR-TOF-MS) in monitoring the kinetics of disinfectant decay in water with a sensitivity one to three orders of magnitude greater than other analytical methods. Chemical disinfection inactivates pathogens during water treatment and prevents regrowth as water is conveyed in distribution system pipes, but it also causes formation of toxic disinfection by-products. Analytical limits have hindered kinetic models, which aid in ensuring water quality and protecting public health by predicting disinfection by-products formation. PTR-TOF-MS, designed for measuring gas phase concentrations of organic compounds, was able to simultaneously monitor aqueous concentrations of five inorganic haloamines relevant to chloramine disinfection under drinking water relevant concentrations. This novel application to aqueous analytes opens a new range of applications for PTR-TOF-MS.

The adoption of drinking water disinfection in the early twentieth century has made waterborne disease outbreaks rare. However, the ability to predict the decay of disinfectants and formation of toxic disinfection by-products (DBPs) has remained a vexing issue[1,2]. A recent paper indicated that 9-45 million Americans are affected annually by health-based water quality violations[3]. Most violations are due to coliform bacteria (37%) and DBP rule violations (25%). A common way to address these issues is to use inorganic chloramines as secondary disinfectants because they form fewer regulated DBPs and persist longer in water distribution systems[4,5]. Considerable work has been done since the 1980s to develop robust kinetic models for chloramine decay[6] and DBP formation[7] in drinking water, but an aspect that is an elusive and emerging issue in such models is the role of bromide (Br^-) in source waters[8]. The presence of Br^- leads to the formation of brominated haloamines and brominated DBPs which are more toxic than their chlorinated counterparts and are often the driver of overall human toxicity[9]. With increasing salinity in freshwaters and the use of alternative, high Br^- source waters (for example, seawater, municipal wastewater), accurate measurements of haloamines are needed to develop reliable models for the formation and transformation of brominated species in drinking water[10,11]. The objectives of this work are to (1) demonstrate that proton transfer time-of-flight mass spectrometry (PTR-TOF-MS) can be used to measure concentrations of trace volatile analytes in the liquid phase and (2) show the methodology can be used to monitor haloamine reactions in real time to expand our knowledge and prediction capabilities of haloamine formation and decay.

Most US drinking water plants utilize two disinfection periods: primary for inactivating microorganisms and secondary for preventing (re)growth of pathogens in water distribution systems. Chloramines are generally formed by first adding free chlorine (prechlorination)

[1]Maseeh Department of Civil, Architectural and Environmental Engineering, University of Texas at Austin, Austin, TX, USA. [2]Office of Research and Development, United States Environmental Protection Agency, Cincinnati, OH, USA. [3]These authors contributed equally: Samuel H. Brodfuehrer, Daniel C. Blomdahl. e-mail: lynnkatz@mail.utexas.edu

for primary disinfection followed by ammonia to form chloramines as secondary disinfectants[12]. For pH ranges typical of drinking water (pH 7 to 9), monochloramine (NH_2Cl) is the most abundant chloramine species; dichloramine ($NHCl_2$) also forms but at lower concentrations[6]. When Br^- is present in source waters monobromamine (NH_2Br), dibromamine ($NHBr_2$) and bromochloramine (NHBrCl) can form. These brominated inorganic haloamines decay more rapidly[13,14] and form greater concentrations of brominated DBPs[15]. The relevant reaction kinetics among these five inorganic haloamines and in waters containing natural organic matter (NOM), the precursor to DBPs, are complex and incompletely understood and yet are a prerequisite for developing mechanistic kinetic models to understand disinfectant residual maintenance, minimize brominated DBP formation and manage water distribution systems in a manner that ensures public health.

A major limitation to the study of chloramine chemistry has been the lack of an analytical method that can in real time accurately measure all relevant inorganic haloamines at concentrations relevant to drinking water[16–18]. Current analytical methods for measuring haloamines are ultraviolet–visible (UV–vis) spectroscopy, colorimetric tests and membrane introduction mass spectrometry (MIMS). UV–vis spectroscopy has been used to study haloamine chemistry but requires concentrations greater than in drinking water and overlapping UV spectra make it difficult to resolve quantitatively when multiple species are present[19,20]. The indophenol[21] and total chlorine N,N-diethyl-p-phenylenediamine (DPD)[22] colorimetric methods are widely employed by water utilities. Whereas these two methods are often used in combination, the results can be confounding; the indophenol method specifically measures NH_2Cl, whereas the total chlorine DPD method measures the total oxidant concentration, which, in the case of chloraminated waters, is the total haloamine concentration on a halogen basis ($[NH_2Cl] + 2[NHCl_2] + [NH_2Br] + 2[NHBrCl] + 2[NHBr_2]$). MIMS uses a semipermeable hydrophobic membrane that rejects water to introduce dissolved analytes to a mass spectrometer that identifies and quantifies analytes based on their mass to charge ratio (m/z). MIMS configurations generally use an electron ionization (EI) source, which generates many fragment ions from the parent molecule. In haloamine systems, this fragmentation results in dihaloamines ($NHCl_2$, $NHBr_2$ and NHBrCl) interfering with the quantification of monohaloamines (NH_2Cl and NH_2Br)[23,24].

PTR-TOF-MS is an analytical technique that uses chemical ionization with hydronium ion (H_3O^+) to measure gas phase volatile organic compounds (VOCs) and inorganic compounds at single parts per trillion concentrations[25]. Chemical ionization is a 'soft ionization' process that results in substantially less fragmentation than EI because less energy is imparted on the parent compound[26,27]. PTR-TOF-MS has been used to measure chloramines in the air at indoor pools[28] and following cleaning with chlorine-based cleaners[29,30]. Selected ion flow tube mass spectrometry, a similar technology to PTR-TOF-MS, has been used to detect and characterize NH_2Cl, $NHCl_2$ and NH_2Br in human breath[31]. The impressive sensitivity of PTR-TOF-MS for measuring gas phase compounds has the potential for correlating gas and aqueous concentrations of haloamines.

In this work, we demonstrate expanded functionality of PTR-TOF-MS by using it to examine drinking water relevant concentrations of inorganic haloamines in real time, thus enabling us to simultaneously quantify aqueous concentrations of haloamines as they form and decay. The data acquired using PTR-TOF-MS enables estimation of relevant kinetic parameters, assessment of relevant competing reactions and validation of any already developed kinetic model. More generally, we show that PTR-TOF-MS can be used to measure concentrations of trace volatile analytes in a liquid phase via headspace analysis, thereby exposing the potential for a wide range of new applications.

Mass spectra of haloamines using PTR-TOF-MS

The protonated molecular ions used for quantification of haloamines were m/z 51.995 (NH_2ClH^+), 85.956 ($NHCl_2H^+$), 95.944 (NH_2BrH^+), 131.903 ($NHBrClH^+$) and 175.852 ($NHBr_2H^+$) because they were the dominant ions. In the mass spectrum for each haloamine (Fig. 1), the protonated molecular ion for acetone, $C_3H_6OH^+$ (m/z 59.049) and acetic acid, $C_2H_4O_2H^+$ (m/z 61.028), are present because they are ubiquitous in the ambient air of indoor spaces and captured due to the open headspace sampling method utilized in this work[29]. PTR-TOF-MS sampling of ambient air in the laboratory contained peaks corresponding to acetone and acetic acid (Supplementary Fig. 1). Additionally, the $NHCl_2$ and NHBrCl mass spectra (Fig. 1b,d) have large peaks of the protonated ion of acetic acid because those experiments were buffered with acetate and performed at pH 4 and 5, respectively.

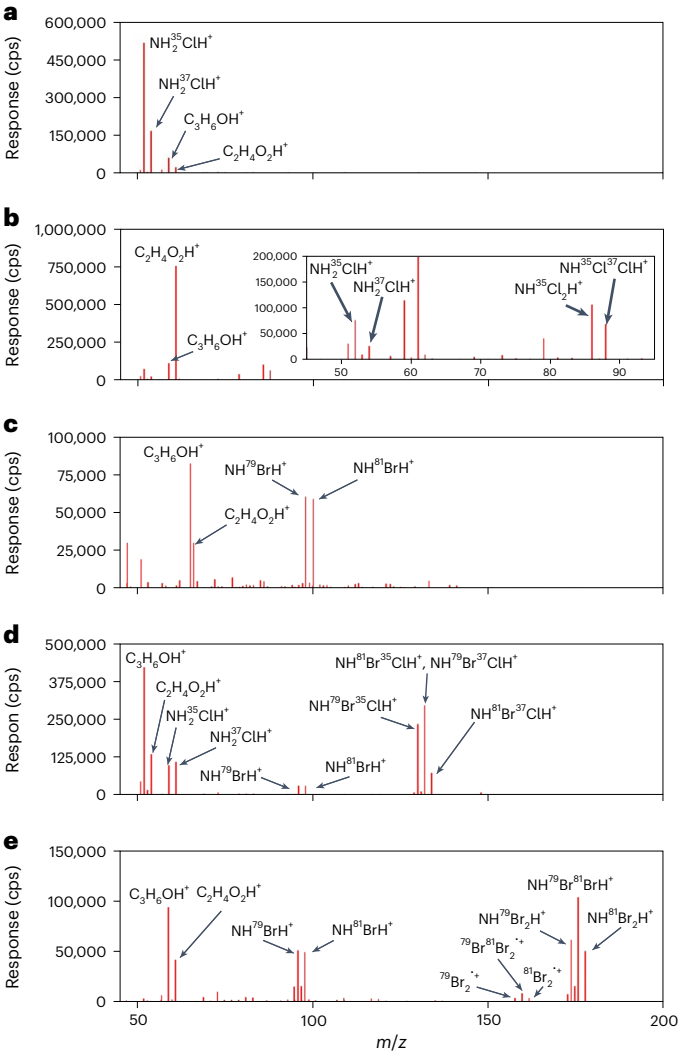

Fig. 1 | Representative PTR-TOF-MS mass spectra for each haloamine. a, 200 µM NH_2Cl. **b**, Mixture of 200 µM $NHCl_2$ and 20 µM NH_2Cl. The $NHCl_2$ standard is present in solution with NH_2Cl. **c**, 50 µM NH_2Br. **d**, Mixture of 200 µM NHBrCl and 100 µM NH_2Cl. Synthesis of a high purity aqueous solution of NHBrCl is impossible, so it must be present in solution with NH_2Cl. **e**, 116 µM $NHBr_2$. cps, counts per second.

The mass spectrum for NH_2Br featured the molecular ions $NH_2{}^{79}BrH^+$ (m/z 95.944) and $NH_2{}^{81}BrH^+$ (m/z 97.942) (Fig. 1c). The mass spectrum for $NHBr_2$ (Fig. 1e) additionally revealed the expected molecular ions $NH^{79}Br_2H^+$ (m/z 173.854), $NH^{79}Br^{81}BrH^+$ (m/z 175.852) and $NH^{81}Br_2H^+$ (m/z 177.851) and the molecular ions of many potential fragment ions, including $NH^{79}BrH^+$ (m/z 94.936), $NH^{81}BrH^+$ (m/z 96.935), $^{79}Br_2{}^{\cdot+}$ (m/z 157.837), $^{79}Br_2{}^{81}Br^{\cdot+}$ (m/z 159.834), $^{81}Br_2{}^{\cdot+}$ (m/z 161.832), $NH^{79}Br_2^+$ (m/z 172.842) and $NH^{79}Br^{81}Br^+$ (m/z 174.842). With EI, the signals for $Br_2{}^{\cdot+}$ ions have been twofold[23] and tenfold[24]

Table 1 | Protonated parent ions detected by PTR-TOF-MS and their mass defects compared to exact values

Haloamine	Ion formula	Isotopic ratio	Exact *m/z*	Detected *m/z*	Mass error (ppm)
Monochloramine	**$NH_2{}^{35}ClH^+$**	**1.00**	**51.99485**	**51.9945**	**6.73**
	$NH_2Cl^{37}H^+$	0.32	53.99190	53.9919	0.00
Dichloramine	**$NH^{35}Cl_2H^+$**	**1.00**	**85.95588**	**85.9564**	**6.05**
	$NH^{35}Cl^{37}ClH^+$	0.64	87.95293	87.9524	6.03
Monobromamine	**$NH_2{}^{79}BrH^+$**	**1.00**	**95.94434**	**95.9438**	**5.63**
	$NH_2{}^{81}BrH^+$	0.97	97.94229	97.9422	0.92
Bromochloramine	$NH^{35}Cl^{79}BrH^+$	0.77	129.90537	129.904	10.55
	$NH^{37}Cl^{79}BrH^+$, $NH^{35}Cl^{81}BrH^+$	**1.00**	**131.90309**	**131.903**	**0.68**
	$NH^{37}Cl^{81}BrH^+$	0.24	133.90037	133.9	2.76
Dibromamine	$NH^{79}Br_2H^+$	0.51	173.85485	173.854	4.89
	$NH^{79}Br^{81}BrH^+$	**1.00**	**175.85280**	**175.852**	**4.55**
	$NH^{81}Br_2H^+$	0.49	177.85075	177.851	1.41
Acetone	$C_3H_6OH^+$	–	59.04914	59.0492	1.02
Acetic Acid	$C_2H_4O_2H^+$	–	61.02840	61.0284	0.00
Trichloramine	$N^{35}Cl_3H^+$	1.00	119.90700	119.9169	82.63
	$N^{35}Cl_2{}^{37}ClH^+$	0.96	121.96000	121.914	377.66
Tribromamine	$NH^{79}Br_3H^+$	0.34	251.76500	251.7654	1.44
	$NH^{79}Br_2{}^{81}BrH^+$	1.00	253.76300	253.7633	1.24
	$NH^{79}Br^{81}Br_2H^+$	0.97	255.76100	255.7613	1.05

Dominant ions in bold. The trihaloamine species were detected but not quantified.

as high as the signal for $NHBr_2$, whereas with PTR-TOF-MS, it is only a tenth of $NHBr_2$, highlighting the cleaner mass spectrum obtained with PTR-TOF-MS versus EI with MIMS. Additional discussion about the mass spectra of the other haloamines is presented in the Supplementary Material (Supplementary Information under 'Discussion of mass spectra for NH_2Cl, $NHCl_2$, NHBrCl').

The expected isotopic ratios and characteristic mass defects of the haloamines detected by the PTR-TOF-MS led to high confidence of ion identification (within >1 mDa mass accuracy). The high resolution (five decimal points, simplified by rounding to three decimal points in this work) *m/z* for molecular and fragment ions and the relative mass error (equation (1)) for all five haloamine isotopes were quantified (Table 1). The average mass deviation for the haloamines detected was 4.73 ± 2.14 ppm, which shows high confidence of ion identification because ions with same nominal mass values can be resolved separately.

$$\text{relative mass error (ppm)} = \frac{m/z_{\text{detected}} - m/z_{\text{exact}}}{m/z_{\text{exact}}} \times 10^6 \quad (1)$$

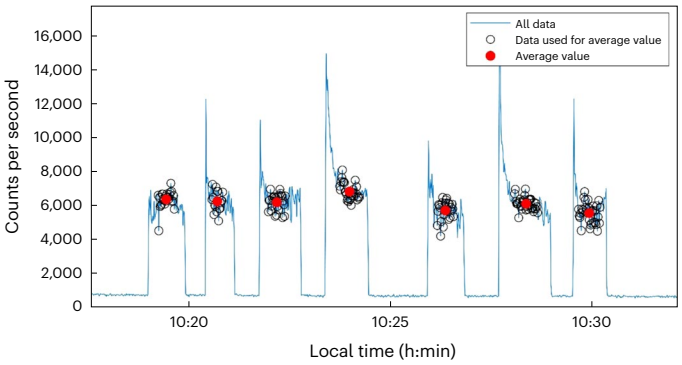

Fig. 2 | PTR-TOF-MS signal counts per second NH_2Cl of seven replicate 2 µM standards. Black circles indicate the periods in each measurement that were averaged into each red data point. Typically, each measurement consisted of a large spike in signal before stabilizing within 20–30 seconds.

As expected, the mass spectra acquired using PTR-TOF-MS were simpler, had fewer fragment ions and contained more distinct peaks for parent ions than those captured using EI. Fragment ions still formed even though chemical ionization with H_3O^+ is a much lower energy process than EI. Some fragments were probably formed due to impurities in the chemical ionization process, which results in the small formation of O_2^+ as part of the ionization gas, which imparts more energy than H_3O^+[28]. The impact of the fragment ions from $NHCl_2$, NHBrCl and $NHBr_2$ on the quantification of NH_2Cl and NH_2Br is further explored in Impact of dihaloamine fragments section.

Dynamic response of sampling and sensitivity analysis

Haloamines concentrations were measured by placing the inlet just above the liquid surface in the aliquot vial which enabled a discrete signal to be measured because the system was open so there was no accumulation of haloamines during sampling. The inlet was typically held there for 30–60 seconds, depending on if a standard or kinetic experiment was being sampled. The PTR-TOF-MS response was immediate with a short-lived spike in haloamine signal that dissipated in less than 5 seconds before stabilizing to a tail with a more consistent instrument response (Fig. 2). Once sampling ended, the signals for corresponding haloamine dissipated immediately. We attribute the short-lived high signal to mixing and increased volatilization resulting from the pipette action into the small vial. The stable tail following the spike is due to a consistent emission of haloamine from the aqueous solution, which is acting as an infinitely large reservoir during the discrete sampling periods, and because the system is open, the volatilized haloamines are not accumulating. Therefore, what is actually being measured is not an equilibrium between the liquid–gas phase but an instantaneous emission rate where the driving force is the haloamine concentration in solution. This is supported by linear agreement in the

standard curves that are discussed in Calibration curves and detection limits section.

To assign a discrete counts per second value for each sampling, we manually selected the period with the stabilized response and averaged it into data points based on the real-time stability of the haloamine PTR-TOF-MS signal. The effectiveness of the manual approach was assessed in a sensitivity analysis that was performed on the data used to develop the standard curves in Supplementary Information under 'Standard curves for haloamines' and the kinetic experiments in Monitoring dynamic aqueous haloamine kinetics section. The sensitivity analysis found that the manual averaging approach had little difference in signal compared to a standardized timing approach. We compared the values of the NH_2Cl and NHBrCl (two haloamines with different volatilities) in the calibration curve and kinetic experiments.

During the calibration curve routine, we compared the manual averaging approach with averaged data between three standardized time periods: the average of signal 10–40 seconds after the inlet was placed into the vial headspace, 10–30 seconds and 20–40 seconds. The calibration sensitivity values and R^2 values had good agreement. Compared with the manual averaging NHBrCl sensitivity of 1,640 cps is counts per second (cps) μM^{-1}, the 10–40 second procedure had a sensitivity of 1,700 cps μM^{-1}, the 10–30 second procedure was 1,750 cps μM^{-1} and the 20–40 second procedure was 1,640. The calibration curve R^2 for each averaging procedure was at least 0.993. NH_2Cl had similar agreement (Supplementary Table 1).

The kinetic experiments required shortening the sampling period to 20–30 seconds to ensure the rate of headspace samples could effectively track the aqueous concentration dynamics. Similar sensitivity analysis was done by comparing the manually averaged data with standardized data averaged from the 10–30 second period after the inlet was placed into the headspace, the 10–20 second period and the 20–30 second period. The standardized data points agreed well with the manual data points, particularly the 20–30 second period as there was more time allowed for the signal to stabilize before the averaging period began. The 20–30 second time period from sampling to counts per second response is fast relative to the common colorimetric methods used for measuring haloamines, which require reactions that take 1 or 5 minutes before quantification. Over the 30-minute kinetic experiments, the mean ratio of the 10–20 second averaging period to the manual period was 1.04 ± 0.062, the mean ratio of the 10–30 second averaging period to the manual period was 1.02 ± 0.040 and the mean 20–30 second averaging period to the manual period was 0.995 ± 0.030.

In both the calibration sampling and the kinetic experiment sampling, the averaging period in each headspace data point (20–40 seconds in the calibration curve, 20–30 seconds in the kinetic experiments) matched the manual averaging and had the most stable signal period as the liquid–gas interface stabilized to a steady emission rate after being pipetted into the sample vial. This observed consistency between both the calibration curve sampling and kinetic experiments over a range of haloamine concentration demonstrates that the kinetics of the haloamine entering vapour phase are not limiting. In future experiments, we recommend averaging in the later, stable period, albeit dependent on the reaction design.

Calibration curves and detection limits

Calibration curves (Supplementary Fig. 2) for each haloamine were successfully developed (discussion in Supplementary Information under 'Standard curves for haloamines'), which demonstrates that PTR-TOF-MS can be used to effectively quantify aqueous haloamine concentrations with headspace measurements over a wide range of drinking water relevant concentrations. The linear correlations that were developed for all haloamines over a wide range of conditions demonstrates that partitioning between the gas and liquid phase is not a limitation of the headspace sampling method because if it was, deviation from linear behaviour would be expected. This result supports the discussion in Dynamic response of sampling and sensitivity analysis section that a steady emission rate during the sampling periods is what is being quantified as opposed to a true equilibrium between the liquid and gas phase. More broadly the results show that PTR-TOF-MS can be used to measure aqueous concentrations. This opens the potential for much broader applications of PTR-TOF-MS technology to quantify low concentrations of volatile compounds in aqueous solutions.

The level of detection (LOD) and level of quantification (LOQ) using PTR-TOF-MS were determined for each haloamine (Supplementary Table 2). The LOD and LOQ were estimated by the method of blank determination where the average haloamine concentration of ten sample blanks plus three and ten times the standard deviation, respectively, for LOD and LOQ[32]. The LODs of NH_2Cl, $NHCl_2$, NH_2Br, NHBrCl and $NHBr_2$ were 0.90, 0.0023, 0.059, 0.0086 and 0.00072 μM. The LOQs of NH_2Cl, $NHCl_2$, NH_2Br, NHBrCl and $NHBr_2$ were 1.1, 0.0045, 0.092, 0.016 and 0.0016 μM. The lowest LODs determined for EI with MIMS for NH_2Cl, $NHCl_2$, NH_2Br, NHBrCl and $NHBr_2$ were 0.48, 0.24, 1.44, 2.51 and 0.84 μM, respectively[24]. PTR-TOF-MS has LODs one to three orders of magnitude lower than EI for all haloamines except NH_2Cl. The improved sensitivity for the haloamines other than NH_2Cl is particularly important because they are present at much lower concentrations than NH_2Cl in chloraminated waters.

Impact of dihaloamine fragments

The dihaloamines ($NHCl_2$, NHBrCl and $NHBr_2$) have been shown to form fragments (Mass spectra of haloamines using PTR-TOF-MS section) that contribute to the molecular ions for NH_2Cl (m/z 51.995) and NH_2Br (m/z 95.944). The contribution from dihaloamines to the fragments at m/z 51.995 and 95.944 must be accounted for to ensure all haloamines are accurately quantified in a mixture. A set of interference calibration curves was developed to account for contribution of the fragment ions from $NHCl_2$, NHBrCl and $NHBr_2$ to those two m/z values (Fig. 3). All the interference calibration curves were fit linearly ($R^2 > 0.92$) with an intercept of zero, except for $NHCl_2$ (Fig. 3a). The non-zero intercept for $NHCl_2$ is probably due to small amounts of HOCl (which can be present at the low pH value of 4 that $NHCl_2$ was formed in this work) being ionized and interfering at m/z 51.995. This phenomenon did not impact the NHBrCl interference calibration curve (Fig. 3b) because less HOCl would be present at the higher pH of 5 and HOCl would rapidly react with Br^- present in the NHBrCl solutions.

PTR-TOF-MS has much lower levels of fragmentation than EI, which makes it a more viable option for collecting robust kinetic data of haloamines. The contribution of 10 μM of dihaloamines to the signals of monohaloamines for PTR-TOF-MS and EI is compared in Table 2. The fragments formed during chemical ionization using PTR-TOF-MS are approximately 2 to 20% of those formed from EI with MIMS. The much lower level of fragmentation of NHBrCl and $NHBr_2$ is particularly important because these dihaloamines can be present in much greater concentrations than $NHCl_2$ in solutions containing Br^-.

Monitoring dynamic aqueous haloamine kinetics

Whereas the preceding discussion highlighted the ability to accurately measure haloamine compounds at environmentally relevant concentrations, a primary goal of this work is to demonstrate the potential for this method to guide model development and predict haloamine formation and decay. Two kinetic experiments were performed, with and without NOM (the major precursor to DBPs found in all source water), to evaluate the effectiveness of using PTR-TOF-MS to measure haloamines in a dynamic mixture. Experiments were designed to simulate the chloramination process used in practice; chloramines are commonly formed with prechlorination followed one minute later by ammonia addition to form chloramines. During each experiment, PTR-TOF-MS was used to simultaneously monitor the five inorganic

https://doi.org/10.1038/s44221-024-00227-4

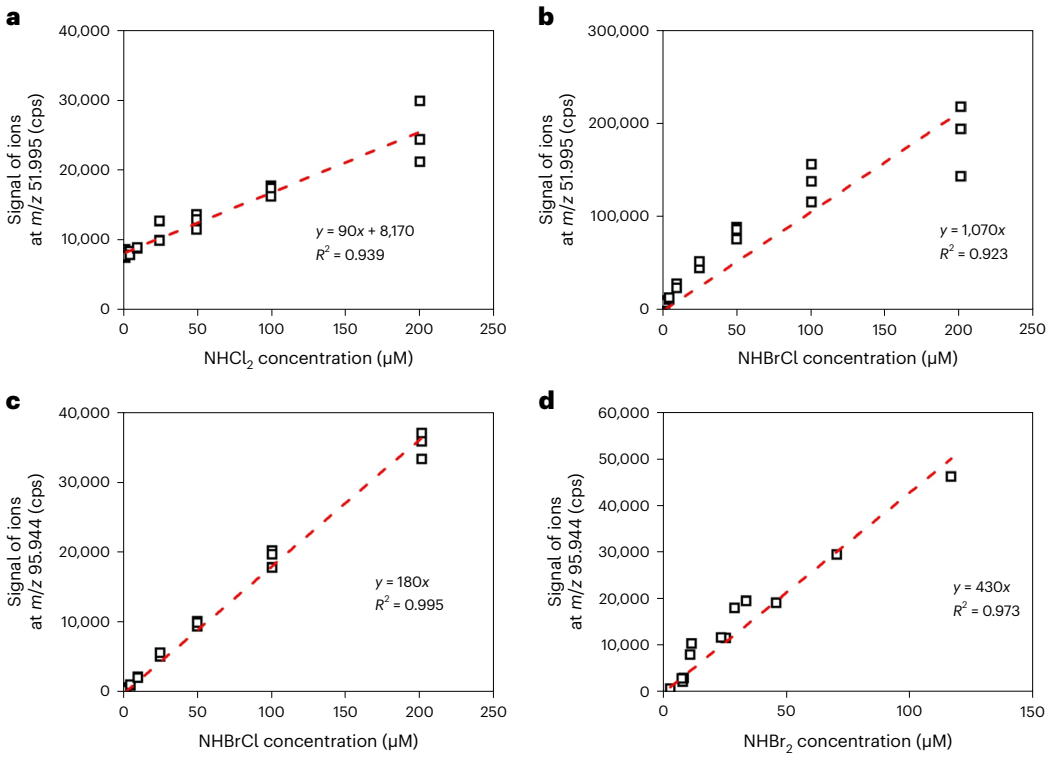

Fig. 3 | Interference from dihaloamines on monohaloamines. a, $NHCl_2$ fragments interfering with NH_2Cl quantification (m/z = 51.995). **b**, NHBrCl fragments interfering with NH_2Cl quantification (m/z = 51.995). **c**, NHBrCl fragments interfering with NH_2Br quantification (m/z = 95.944). **d**, $NHBr_2$ fragments interfering with NH_2Br quantification (m/z = 95.944).

Table 2 | Contribution of 10 μM of dichloramine ($NHCl_2$), bromochloramine (NHBrCl) and dibromamine ($NHBr_2$) to signals associated with monochloramine (NH_2Cl) and monobromamine (NH_2Br) comparison between PTR-TOF-MS and EI with MIMS

	PTR-TOF-MS (this work)		EI (Pope[23])		EI (Hu et al.[24])	
Dihaloamine	NH_2Cl	NH_2Br	NH_2Cl	NH_2Br	NH_2Cl	NH_2Br
$NHCl_2$	0.3 μM	-	17 μM	-	5.2 μM	-
NHBrCl	3.2 μM	1.4 μM	50 μM	7.8 μM	NM*	NM*
$NHBr_2$	-	3.4 μM	-	28 μM	-	21 μM

*NM, not measured.

haloamines studied. The indophenol and total chlorine DPD colorimetric methods were also used to measure NH_2Cl and total haloamine ($[NH_2Cl] + 2[NHCl_2] + [NH_2Br] + 2[NHBrCl] + 2[NHBr_2]$) concentrations, respectively.

The effectiveness of using PTR-TOF-MS for monitoring haloamine concentrations was assessed by comparing the results to the colorimetric methods in both kinetic experiments. The NH_2Cl and total haloamine concentrations measured using PTR-TOF-MS were in good agreement with those determined with the established colorimetric methods with differences ranging from 0.4 to 3.7 μM (4.1 to 13%) for the experiment without NOM (Fig. 4a) and 0.03 to 6.2 μM (0.1 to 37%) for the experiment with NOM (Fig. 4b). The consistency between the two total haloamine measurements shows that the mass balance on the haloamines measured using PTR-TOF-MS is correct. Accurate NH_2Cl measurements highlight the ability to account for fragment ions because the most relevant impact of fragmentation occurs when NHBrCl interferes with NH_2Cl quantification (Table 2) and NHBrCl forms rapidly during the kinetic experiments (Fig. 5). Additionally, the consistency between the PTR-TOF-MS and colorimetric method measurements in the NOM experiment shows that a low concentration of organic carbon (2 mg l^{-1} as C), typical of natural waters, does not meaningfully impact or interfere with the PTR-TOF-MS method for quantifying haloamines.

Implications for existing haloamine models

The kinetic experiment monitored by PTR-TOF-MS shows that in the absence of NOM, the concentrations of the various haloamines changed substantially during the short 30-minute experiments (Fig. 5). NH_2Cl and NH_2Br were rapidly consumed to form NHBrCl and $NHBr_2$ and the dihaloamines then decayed. $NHCl_2$ was excluded from Fig. 5 because it was present at very low concentrations (<0.1 μM) and did not change substantially. The experimental data were also compared to the most widely used haloamine model (Fig. 5 and Supplementary Table 3) and another model developed by Pope using MIMS (Supplementary Fig. 3 and Supplementary Table 4). The two kinetic models yield similar simulated concentrations of haloamines; therefore, we will focus on the comparison to the kinetic model developed by Luh and Mariñas (L&M model)[20]. More recent studies have been performed to better understand bromamine chemistry, but they have not been incorporated into the existing inorganic haloamine models[13,33].

Substantial discrepancies are apparent between the L&M model and the data collected using PTR-TOF-MS, which highlights the major deficiencies in existing kinetic models to describe haloamine formation and decay at conditions representative of actual chloramine application to drinking water (for example, pH 7–9, <4 mg Cl_2 l^{-1} and chloramines formed with a prechlorination step). The L&M model greatly underpredicts NH_2Cl decay and NHBrCl formation, while also overpredicting $NHBr_2$ formation. The predicted dominant brominated haloamine was $NHBr_2$ whereas the PTR-TOF-MS data showed that NHBrCl was the dominant brominated haloamine after the first

https://doi.org/10.1038/s44221-024-00227-4

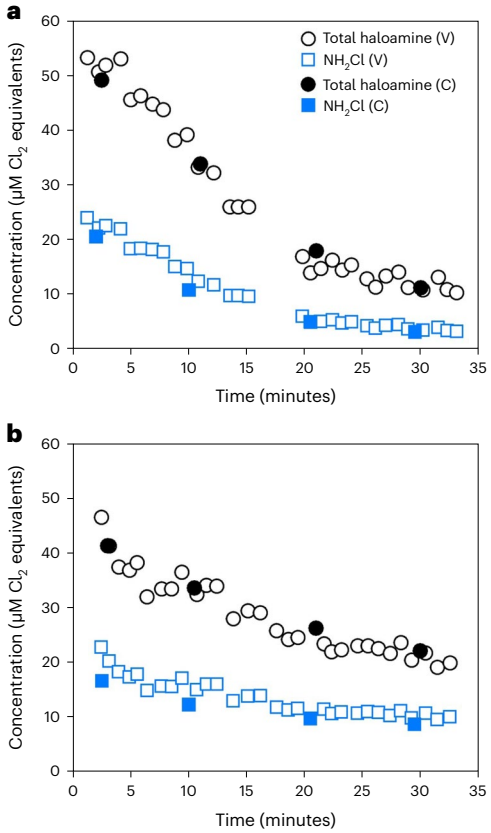

Fig. 4 | Measured concentrations of total haloamines and monochloramine. Measured concentrations of total haloamines and monochloramine during kinetic experiment using PTR-TOF-MS (V) and colorimetric (C) methods. pH 7.2, 10 mM phosphate buffer and $[Br^-]$ = 2 mg l^{-1} as Br^- (25 μM) dosed with [HOCl] = 4 mg l^{-1} as Cl_2 (56 μM) for 1 minute followed by addition of $[NH_3]$ = 1.3 mg l^{-1} as N (93 μM). **a**, Without NOM. **b**, [NOM] = 2 mg l^{-1} as C.

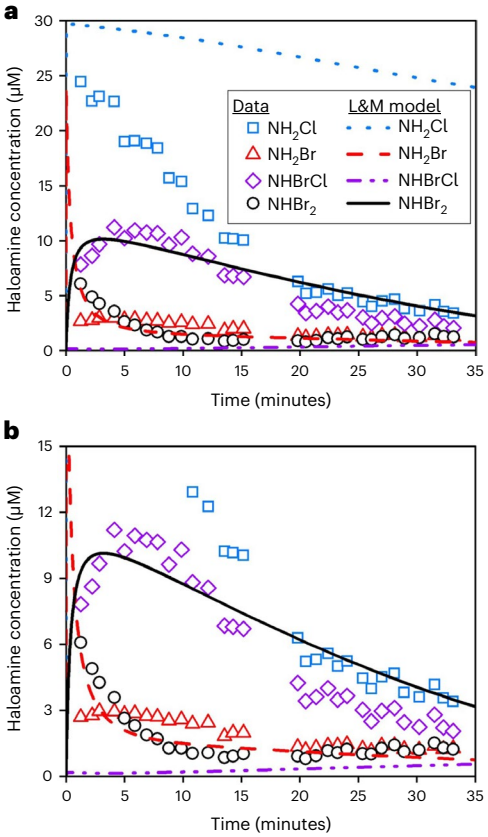

Fig. 5 | Comparison of model to measured haloamine concentrations during the kinetic experiment using PTR-TOF-MS. Comparison of Luh and Mariñas[20] model (lines) to measured (points) haloamine concentrations during the kinetic experiment using PTR-TOF-MS. pH 7.2, 10 mM phosphate buffer and $[Br^-]$ = 2 mg l^{-1} as Br^- (25 μM) dosed with [HOCl] = 4 mg l^{-1} as Cl_2 (56 μM) for 1 minute followed by addition of $[NH_3]$ = 1.3 mg l^{-1} as N (93 μM). **a**, 0–30 μM concentration range. **b**, 0–15 μM concentration range. L&M, Luh and Mariñas.

two minutes. Therefore, if one relied on the L&M model to understand brominated DBP formation, the model estimated dominant brominated haloamine, $NHBr_2$, could be incorrectly associated with DBP formation instead of NHBrCl.

The differences between the L&M model and PTR-TOF-MS data reflect the limitations of current analytical methods, which required Luh and Mariñas to perform experiments at conditions atypical of chloramination. They combined NH_2Cl (at a concentration more than threefold higher than the highest allowable chloramine concentration of 4 mg Cl_2 l^{-1} in drinking water) with a fivefold excess of Br^- to form NHBrCl (example shown in Supplementary Fig. 4). This approach resulted in a set of reactions that applies to their experimental conditions but does not translate to more representative chloramination conditions as exhibited in Fig. 5. PTR-TOF-MS can overcome the previous issues by providing more representative experimental data to develop a truly comprehensive haloamine kinetic model for guiding and optimizing disinfection practices when using chloramines. Additionally, PTR-TOF-MS can monitor the relevant haloamine species when NOM is present which is advantageous for studying haloamine reactions with NOM that lead to DBP formation (Supplementary Fig. 5).

Conclusion

The use of PTR-TOF-MS to sample the headspace of an aqueous solution and directly correlate that to dissolved concentrations opens a wide range of new potential uses for this analytical technology. These applications include measurement of reaction kinetics and concentrations in relevant matrices. In addition to examining the broad range of inorganic and organic disinfectant by-products that are challenging to identify and analyse, other examples include the broad range of contaminants that may be present in water reuse and alternative water supplies, advanced oxidation treatment kinetics of pharmaceuticals and personal care products and per- and polyfluoroalkyl substances concentrations and reaction chemistry using different ionization modes. More generally, measurement of VOCs in water requires sample preparation (for example, extractions, concentrating), separation by gas chromatography and then quantification via mass spectrometry, flame ionization detection or electron capture detection[34]. Additional work is necessary to test the effectiveness of PTR-TOF-MS for the wide range of VOCs in water, but the work in this study demonstrated a proof of concept that rapid, sensitive headspace sampling can be used to directly determine aqueous concentrations of volatile analytes in real time. A potential further improvement to the method would be the use of a semipermeable membrane as an introduction phase (that is, MIMS) with PTR-ToF.

The novel haloamine kinetic data collected in this work highlights a particularly useful application of PTR-TOF-MS because not only are aqueous concentrations being measured but reactions kinetics are being assessed in real time. The data demonstrated major deficiencies in existing kinetic models, illustrating their limited usefulness in predicting disinfectant residual maintenance and DBP formation and more broadly as tools for managing water distribution systems.

Because PTR-TOF-MS allows simultaneous, real-time measurement of the five important haloamines, future experimental work and modelling will be able for the first time to evaluate kinetic models for all important species. Additionally, this method has the potential to also study the simultaneous formation of DBPs, which would provide even greater insight into the formation mechanisms of DBPs. Such a study would allow revisions to existing kinetic models to close fundamental knowledge gaps, thereby enabling a better understanding of Br^- impacted waters and providing more robust predictive tools for managing drinking water treatment plants and distributions systems.

Methods

Synthesis of haloamines

Reagent grade chemicals and ultrapure water (18.2 MΩ cm, Milli-Q, Millipore) were used to prepare all stock haloamine solutions and dilutions and wrapped in foil to protect against UV-induced decay. The haloamines were made by combining hypochlorite (OCl^-) or hypobromite (OBr^-) with ammonia chloride (NH_4Cl) at various halogen to nitrogen ratios (X_2/N) and pH values. A 4.99% sodium hypochlorite solution (NaOCl) solution was used to make hypobromite ion (OBr^-) solutions. The OCl^- concentration was determined before use by measuring the absorbance on a Hach DR6000 Spectrophotometer (Hach Company) at 292 nm, using a molar absorptivity ($\varepsilon_{OCl^-,292nm}$) of 362 M^{-1} cm^{-1} (ref. 35). The OBr^- stock solution was prepared by combining OCl^- with Br^- at a Br^-/Cl_2 molar ratio of 1.05. The exact OBr^- stock solution concentration was determined by monitoring the absorbance for OBr^- at 329 nm ($\varepsilon_{OBr^-,329nm}$ = 332 $M^{-1}cm^{-1}$) (ref. 36).

The NH_2Cl stock solution was prepared by adding OCl^- dropwise to a well-mixed pH 9 ammonia solution at a Cl_2/N molar ratio of 0.6. The NH_2Cl stock solution concentration was determined by measuring the absorbance at 243 nm ($\varepsilon_{NH_2Cl,243nm}$ = 461 $M^{-1}cm^{-1}$) (ref. 37). The $NHCl_2$ stock solution was prepared by buffering a NH_2Cl solution with 10 mM acetate and rapidly dropping the pH to 4. The $NHCl_2$ solution was aged for at least 4 hours to maximize formation of $NHCl_2$. The $NHCl_2$ and NH_2Cl concentrations were determined by reconciling overlapping UV spectra at 243 ($\varepsilon_{NH_2Cl,243nm}$ = 461 $M^{-1}cm^{-1}$ and $\varepsilon_{NHCl_2,243nm}$ = 235 $M^{-1}cm^{-1}$) and 294 nm ($\varepsilon_{NH_2Cl,294nm}$ = 15 $M^{-1}cm^{-1}$ and $\varepsilon_{NHCl_2,294nm}$ = 282 $M^{-1}cm^{-1}$).

The NH_2Br stock solution was prepared by combining ammonia and OBr^- solutions at a Br_2/N molar ratio of 1:1000 at pH 9 (the large excess of ammonia buffered the solution). The $NHBr_2$ stock solution was prepared by combining ammonia and OBr^- at a Br_2/N molar ratio of 1:2 at pH 7.2 in 10 mM phosphate buffer. The NH_2Br and $NHBr_2$ concentrations in each stock solution were determined by reconciling overlapping UV spectra at 232 ($\varepsilon_{NH_2Br,232nm}$ = 82 $M^{-1}cm^{-1}$ and $\varepsilon_{NHBr_2,232nm}$ = 2,000 $M^{-1}cm^{-1}$) and 278 nm ($\varepsilon_{NH_2Br,278nm}$ = 425 $M^{-1}cm^{-1}$ and $\varepsilon_{NHBr_2,278nm}$ = 715 $M^{-1}cm^{-1}$) (ref. 38).

The NHBrCl stock solution was prepared by combining a NH_2Cl solution with HOBr at a NH_2Cl/HOBr molar ratio of 3:2 at pH 5 in 10 mM acetate buffer. At these conditions, NHBrCl will rapidly form and is sufficiently stable for analysis within minutes[39]. The NHBrCl concentration was equal to the HOBr added and the NH_2Cl concentration was equal to half the NHBrCl concentration.

PTR-TOF-MS operating parameters and sampling procedure

A Vocus 2 R PTR-TOF-MS (Aerodyne Inc., Billerica) was used to measure haloamine concentrations. Through interactions of H_3O^+ ions with samples, PTR-TOF allows for excellent transmission of volatile compounds whose proton affinity is higher than water. Whereas previous-generation PTR-MS instruments are dependent on humidity[40,41], the Vocus PTR-TOF-MS used has been shown to have no humidity dependency due to the focused ion molecular reactor (FIMR) design. The FIMR is flooded with enough water vapour (in mixing ratios of 20%) that the addition of humid sampled air has a negligible effect[42]. The internal parameters used in PTR-TOF-MS greatly impact ion sensitivities and detection transmission efficiencies[43,44]. The following optimized parameters were used: FIMR pressure = 2.3 mbar, FIMR temperature = 120 °C, big segmented quadrupole voltage = 275 V, H_3O^+ ion source flow rate = 15 sccm, FIMR front voltage = 650 V, FIMR rear voltage = 25 V. These settings resulted in E/N = 155 Td, where E is the electrical field strength and N is the gas number density, which is sufficiently high to prevent excessive water clusters in high humidity samples. The Vocus PTR-TOF-MS also has a quadrupole radio frequency field on the outside of the glass ion molecular reactor, which focusses ions into the centre of the reactor and minimizes wall interactions and losses[42]. The PTR-TOF-MS parameters used in this study are commonly used in studies[45,46] but were further optimized in the current work for NH_2Cl, $NHCl_2$ and NH_2Br signals by adjusting FIMR parameters including temperature.

Headspace sampling was used to measure haloamine concentrations in standards for calibration curves and samples from kinetic experiments (Supplementary Fig. 6). 5 ml of a solution was pipetted from a bulk standard or experiment into a 2 dram (7.4 ml) screw-top vial (Fisherbrand vial N51A, Fisher Scientific Inc.), and a 1/8-inch polytetrafluoroethylene line (length of ~20 cm) was connected to the Vocus inlet and held 1 cm above the liquid surface of the solution (it took approximately 30 seconds to transfer samples for measurement on the PTR-TOF-MS). The Teflon line was held in the vial until the Vocus signal stabilized, approximately 20–30 seconds. The PTR-TOF-MS was operated at 1 Hz time resolution and with sufficient flow pressure (using a LI-COR 850 CO_2 monitor as a pump downline) to result in <1 second response time. Because the volatilization of haloamines from the liquid phase to the gas phase is what is being quantified, this measurement is influenced by the liquid phase temperature. The laboratory has a high air exchange rate of approximately 10 air changes per hour and the temperature is controlled by an heating, ventilation and air conditioning system that provides constant temperature (22 ± 1 C) over the course the experiments. All standard headspace measurements were completed in at least triplicate except in the case of $NHBr_2$, which will be discussed later.

Data processing of the Vocus concentration data was done using PTRwid (version v_003_jul_01_2021) with the configuration file customized to cause all five haloamines and their halogen isotopes to be added to the unified mass list[47]. The protonated m/z ratio (as measured by the Vocus) of the isotopes of each haloamine, volatile buffer and acetone are shown in Table 1. The PTRwid data processing resulted in a concentration time series at 1 Hz time resolution which was further analysed using MATLAB (Mathworks). Headspace sampling was performed until a consistent mass spectrum was observed for 15–20 seconds.

Calibration curves

The NH_2Cl, $NHCl_2$ and NH_2Br stock solutions were used to make a series of dilutions to make standards for calibration of the mass spectrometer. The NHBrCl standards were made by combining NH_2Cl and HOBr for each individual standard. $NHBr_2$ is inherently unstable and rapidly decays so it was impossible to make a series of standards diluted from a stock solution. Therefore, the standard curve for $NHBr_2$ was made by simultaneously monitoring the decaying concentration of the $NHBr_2$ stock solution using UV–vis spectroscopy and then immediately pipetting a sample for analysis. This procedure was then repeated every few minutes on the decaying $NHBr_2$ solution to obtain the data needed to make the $NHBr_2$ calibration curve.

Kinetic experiments

Two kinetic experiments, one without NOM and one with NOM, were performed to assess the effectiveness of using PTR-TOF-MS to measure haloamine mixtures undergoing formation and decay. To maximize brominated haloamine formation, prechlorination used Br^- and free chlorine concentrations at the upper range that occurs in drinking water treatment[8] before ammonia addition to form haloamines. For the experiment without NOM, a solution of 2 mg l^{-1} as Br^- (25 μM) in

10 mM phosphate buffer at pH 7.2 was prepared and dosed with 4 mg l^{-1} as Cl_2 of free chlorine (56 µM). The solution was mixed for 1 minute, the median prechlorination duration[48], and then ammonia was added at a Cl_2/N molar ratio of 0.6 to form haloamines. The same procedure was repeated for the experiment with NOM except that 2 mg l^{-1} as C of Upper Mississippi River NOM (International Humic Substance Society, St Paul, MN, USA) was also present in solution before free chlorine addition. Ammonia addition initiated the start of a kinetic experiment because within milliseconds the monohaloamines, NH_2Cl and NH_2Br, form. Monitoring continued for 30 minutes using PTR-TOF-MS and the indophenol and total chlorine DPD colorimetric methods. Samples were continuously taken from the bulk sample and put in the screw-top vials to be analysed by the PTR-TOF-MS, and samples were taken at approximately 2, 10, 20 and 30 minutes to be analysed using the colorimetric methods.

Data availability

All data supporting the finding of this study are available within this article and its Supplementary Information. The data that support the findings of this study are available via figshare at https://doi.org/10.6084/m9.figshare.25302220 (ref. 49).

References

1. Rosario-ortiz, B. F. et al. How do you like your tap water? *Science* **351**, 912–914 (2016).
2. Sedlak, D. L. & von Gunten, U. The chlorine dilemma. *Science* **331**, 42 LP–43 (2011).
3. Allaire, M., Wu, H. & Lall, U. National trends in drinking water quality violations. *Proc. Natl Acad. Sci. USA* **115**, 2078–2083 (2018).
4. *2017 Water Utility Disinfection Survey Report* (American Water Works Association, 2018).
5. *Monochloramine in Drinking-Water: Background Document for Development of WHO Guidelines for Drinking-Water Quality* (World Health Organization, 2004).
6. Valentine, R. L. & Jafvert, C. T. Reaction scheme for the chlorination of ammoniacal water. *Environ. Sci. Technol.* **26**, 577–586 (1992).
7. Duirk, S. E. & Valentine, R. L. Modeling dichloroacetic acid formation from the reaction of monochloramine with natural organic matter. *Water Res.* **40**, 2667–2674 (2006).
8. Amy, G., Siddigui, M., Zhai, W., DeBroux, J. & Odem, W. *Survey of Bromide in Drinking Water and Impacts on DBP Formation* (Water Research Foundation, 1994).
9. Allen, J. M. et al. Drivers of disinfection byproduct cytotoxicity in U.S. drinking water: should other DBPs be considered for regulation? *Environ. Sci. Technol.* **56**, 392–402 (2022).
10. Dietrich, A. M. & Burlingame, G. A. Critical review and rethinking of USEPA secondary standards for maintaining organoleptic quality of drinking water. *Environ. Sci. Technol.* **49**, 708–720 (2015).
11. Vidic, R. D., Brantley, S. L., Vandenbossche, J. M., Yoxtheimer, D. & Abad, J. D. Impact of shale gas development on regional water quality impact of shale gas development. *Science* **340**, 6134 (2013).
12. Kirmeyer, G., Martel, K., Thompson, G. & Radder, L. *Optimizing Chloramine Treatment* (Water Research Foundation, 2004).
13. Wahman, D. G., Speitel, G. E. & Katz, L. E. Bromamine decomposition revisited: a holistic approach for analyzing acid and base catalysis kinetics. *Environ. Sci. Technol.* **51**, 13205–13215 (2017).
14. Trofe, T. W., Inman, G. W. & Donald Johnson, J. Kinetics of monochloramine decomposition in the presence of bromide. *Environ. Sci. Technol.* **14**, 544–549 (1980).
15. Pope, P. G. & Speitel, G. E. Reactivity of bromine-substituted haloamines in forming haloacetic acids. *ACS Symp. Ser.* **995**, 182–197 (2008).
16. Kinani, S., Roumiguières, A. & Bouchonnet, S. A critical review on chemical speciation of chlorine-produced oxidants (CPOs) in seawater. Part 1: chlorine chemistry in seawater and its consequences in terms of biocidal effectiveness and environmental impact. *Crit. Rev. Anal. Chem.* https://doi.org/10.1080/10408347.2022.2139590 (2022).
17. Kinani, S., Roumiguières, A. & Bouchonnet, S. A Critical review on chemical speciation of chlorine-produced oxidants (CPOs) in seawater. Part 2: sampling, sample preparation and non-chromatographic and mass spectrometric-based methods. *Crit. Rev. Anal. Chem.* https://doi.org/10.1080/10408347.2022.2135984 (2022).
18. Roumiguières, A., Bouchonnet, S. & Kinani, S. A critical review on chemical speciation of chlorine-produced oxidants in seawater. Part 3: chromatographic- and mass spectrometric-based methodologies. *Crit. Rev. Anal. Chem.* https://doi.org/10.1080/10408347.2023.2220129 (2023).
19. Brodfuehrer, S. H., Wahman, D. G., Alsulaili, A., Speitel, G. E. & Katz, L. E. Role of carbonate species on general acid catalysis of bromide oxidation by hypochlorous acid (HOCl) and oxidation by molecular chlorine (Cl2). *Environ. Sci. Technol.* **54**, 16186–16194 (2020).
20. Luh, J. & Mariñas, B. J. Kinetics of bromochloramine formation and decomposition. *Environ. Sci. Technol.* **48**, 2843–2852 (2014).
21. *Method 10020, Chloramine (Mono) and Nitrogen, Free Ammonia* (Hach Company, 2019).
22. *Method 10070, Chlorine, Free and Total, High Range* (Hach Company, 2018).
23. Pope, P. G. *Haloacetic Acid Formation During Chloramination: Role of Environmental Conditions, Kinetics, and Haloamine Chemistry* (University of Texas at Austin, 2006).
24. Hu, W., Lauritsen, F. R. & Allard, S. Identification and quantification of chloramines, bromamines and bromochloramine by membrane introduction mass spectrometry (MIMS). *Sci. Total Environ.* **751**, 142303 (2021).
25. Blake, R. S., Monks, P. S. & Ellis, A. M. Proton-transfer reaction mass spectrometry. *Chem. Rev.* **109**, 861–896 (2009).
26. Thompson, J. M. Introduction. in *Mass Spectrometry* 1–56 (Pan Stanford Publishing Pte., 2018).
27. Roumiguières, A., Bouchonnet, S. & Kinani, S. Challenges and opportunities for on-line monitoring of chlorine-produced oxidants in seawater using portable membrane-introduction Fourier transform-ion cyclotron resonance mass spectrometry. *Anal. Bioanal. Chem.* **413**, 885–900 (2021).
28. Wu, T. et al. Real-time measurements of gas-phase trichloramine (NCl_3) in an indoor aquatic center. *Environ. Sci. Technol.* **55**, 8097–8107 (2021).
29. Arata, C. et al. Volatile organic compound emissions during HOMEChem. *Indoor Air* **31**, 2099–2117 (2021).
30. Bhattacharyya, N. et al. Bleach emissions interact substantially with surgical and KN95 mask surfaces. *Environ. Sci. Technol.* **57**, 6589–6598 (2023).
31. Senthilmohan, S. T. et al. Detection of monobromamine, monochloramine and dichloramine using selected ion flow tube mass spectrometry and their relevance as breath markers. *Rapid Commun. Mass Spectrom.* **22**, 677–681 (2008).
32. Shrivastava, A. & Gupta, V. B. Methods for the determination of limit of detection and limit of quantitation of the analytical methods. *Chron. Young Sci.* **2**, 21–25 (2011).
33. Mensah, A. T., Berne, F., Allard, S., Soreau, S. & Gallard, H. Kinetic modelling of the bromine-ammonia system: formation and decomposition of bromamines. *Water Res.* **224**, 119058 (2022).
34. Demeestere, K., Dewulf, J., De Witte, B. & Van Langenhove, H. Sample preparation for the analysis of volatile organic compounds in air and water matrices. *J. Chromatogr. A* **1153**, 130–144 (2007).

35. Furman, C. S. & Margerum, D. W. Mechanism of chlorine dioxide and chlorate ion formation from the reaction of hypobromous acid and chlorite ion. *Inorg. Chem.* **37**, 4321–4327 (1998).
36. Troy, R. C. & Margerum, D. W. Non-metal redox kinetics: hypobromite and hypobromous acid reactions with iodide and with sulfite and the hydrolysis of bromosulfate. *Inorg. Chem.* **30**, 3538–3543 (1991).
37. Kumar, K., Day, R. A. & Margerum, D. W. Atom-transfer redox kinetics: general-acid-assisted oxidation of iodide by chloramines and hypochlorite. *Inorg. Chem.* **25**, 4344–4350 (1986).
38. Lei, H., Mariñas, B. J. & Minear, R. A. Bromamine decomposition kinetics in aqueous solutions. *Environ. Sci. Technol.* **38**, 2111–2119 (2004).
39. Brodfuehrer, S. H., Goodman, J. B., Wahman, D. G., Speitel, G. E. & Katz, L. E. Apparent reactivity of bromine in bromochloramine depends on synthesis method: implication bromine chloride and molecular bromine as important bromine species. *J. Environ. Eng.* **148**, 12 (2022).
40. de Gouw, J. & Warneke, C. Measurements of volatile organic compounds in the earth's atmosphere using proton-transfer-reaction mass spectrometry. *Mass Spectrom. Rev.* **26**, 223–257 (2007).
41. Warneke, C., van der Veen, C., Luxembourg, S., de Gouw, J. A. & Kok, A. Measurements of benzene and toluene in ambient air using proton-transfer-reaction mass spectrometry: calibration, humidity dependence, and field intercomparison. *Int. J. Mass Spectrom.* **207**, 167–182 (2001).
42. Krechmer, J. et al. Evaluation of a new reagent-ion source and focusing ion–molecule reactor for use in proton-transfer-reaction mass spectrometry. *Anal. Chem.* **90**, 12011–12018 (2018).
43. Blomdahl, D. C. *Optimization of Volatile Organic Compound Sensitivity of Vocus PTR-ToF-MS for Quantifying Disinfection Byproducts* (Univ. Texas at Austin, 2021).
44. Riva, M. et al. Evaluating the performance of five different chemical ionization techniques for detecting gaseous oxygenated organic species. *Atmos. Meas. Tech.* **12**, 2403–2421 (2019).
45. Hall, E. C. et al. Varying humidity increases emission of volatile nitrogen-containing compounds from building materials. *Build. Environ.* **205**, 108290 (2021).
46. Sreeram, A., Blomdahl, D., Misztal, P. & Bhasin, A. High resolution chemical fingerprinting and real-time oxidation dynamics of asphalt binders using Vocus Proton Transfer Reaction (PTR-TOF) mass spectrometry. *Fuel* **320**, 123840 (2022).
47. Holzinger, R. PTRwid: a new widget tool for processing PTR-TOF-MS data. *Atmos. Meas. Tech.* **8**, 3903–3922 (2015).
48. AWWA Disinfection Systems Committee. Committee report: disinfection survey, part—alternatives, experiences, and future plans. *Am. Water Works Assoc.* **100**, 110–124 (2008).
49. Brodfuehrer, S. H. et al. Data for 'Simultaneous time-resolved inorganic haloamine measurement empowers robust analysis of disinfectant degradation kinetics and by-product formation'. *figshare* https://doi.org/10.6084/m9.figshare.25302220 (2024).

Acknowledgements

This work was supported by the National Science Foundation under grant 1953206. The research presented was not performed or funded by EPA and was not subject to EPA's quality system requirements. The views expressed in this article are those of the author(s) and do not necessarily represent the views or the policies of the US Environmental Protection Agency. Any mention of trade names, manufacturers or products does not imply an endorsement by the United States Government or the US Environmental Protection Agency. EPA and its employees do not endorse any commercial products, services or enterprises.

Author contributions

P.K.M. and L.E.K. conceived the research. S.H.B., D.C.B., P.K.M. and L.E.K. designed the research. S.H.B. and D.C.B. performed the experimental work. S.H.B., D.C.B., D.G.W., G.E.S., P.K.M. and L.E.K. contributed to interpreting the data. S.H.B. and D.C.B. wrote the original draft. S.H.B., D.C.B., D.G.W., G.E.S., P.K.M. and L.E.K. contributed to reviewing and editing the manuscript.

Competing interests

The authors declare no competing interests.

Additional information

Supplementary information The online version contains supplementary material available at https://doi.org/10.1038/s44221-024-00227-4.

Correspondence and requests for materials should be addressed to Lynn E. Katz.

Peer review information *Nature Water* thanks Said Kinani and the other, anonymous, reviewer(s) for their contribution to the peer review of this work.